

A Comparative Study of Wind Energy Conversion System incorporating the Doubly Fed Induction Generator and the Permanent Magnet Synchronous Generator

Welcome Khulekani Ntuli and Musasa Kabeya
Durban University of Technology, Durban, South Africa
kwntuli8@gmail.com, musasak@dut.ac.za

Gulshan Sharma
University of Johannesburg, Johannesburg, South Africa
gulshanmail2005@gmail.com

Abstract

The renewable energy power producer (RPP) sector is growing rapidly to become an important source of power in South Africa and in nations across the globe. Companies within this sector provide a variety of clean energy sources. Despite its ability to support the power system and conserve the environment that sustains life, the rising usage of renewable distributed generators (RDGs) poses power quality problems in the overall distribution network, such as the voltage instability at buses, the increase in voltage/current harmonic distortions, etc. Furthermore, RDGs are required to remain connected to the electrical power network during grid faults and provide system support by injecting reactive current when required, depending on the nature of the fault. This study provides a dynamic performance analysis of a doubly fed induction generator (DFIG) based wind energy conversion system (WECS), and permanent magnet synchronous generator (PMSG) based WECS. The potential fault ride-through capability solutions in grid code power generation and injection of reactive power are taken into account, and the application results of both systems are shown under similar working conditions. From the simulation results, it is found that the DFIG based WECS topology performed well compared to the PMSG based WECS topology.

Keywords: Fault-ride through capability, doubly fed induction generator, permanent magnet synchronous generator, wind energy conversion system.

1. Introduction

In this contemporary region, the contribution of thermal power plants to environmental pollution and global warming has become a serious economic issue. This has led academics to look for ways to generate electricity without using carbon as an alternative to the ways that are currently used (Qazi et al., 2019), (Olson-Hazboun, 2018). Wind energy conversion systems (WECS) are one of the most enticing renewable distributed generators (RDGs) due to their broad availability and the financial benefits associated with high power generation (McKenna et al., 2022). This RDG can be categorized into two technologies: doubly fed induction generator (DFIG)-based WECS, or permanent magnet synchronous generator (PMSG)-based WECS (Gupta & Shukla, 2022), (Ouyang et al., 2019), (Nadour et al., 2020). The increasing use of RDGs poses power quality problems in the overall distribution network, such as the voltage instability at buses, the increase in voltage/current harmonic distortions, etc., despite their ability to support the power system and preserve the environment that sustains life. The standard grid code defines the technical standards for connecting RDGs to the power system to assure the safety, security, and proper operation of the entire power system. Grid code specifications include the limit of voltage variations (i.e., ± 1 pu), the limit of frequency variations (i.e., $\pm 5\%$), the limit of current/voltage harmonic distortions (i.e., total harmonic distortion voltage (THD_v) of 0.1% and total harmonic distortion current (THD_i) of 5%),

and the limit of power factor (i.e., Pf = 0.9-0.95), (Voglitsis et al., 2016).

In the past, if there was a problem with the power grid, RDGs could be disconnected from it avoid serious damage. Nevertheless, in the present day, RDGs are expected to remain connected during grid failure and provide grid support. Grid code requirements are used to effectively describe the technical details of RDGs that are connected to the power system (Sewchurran & Davidson, 2016). In accordance with South Africa technical grid-code regulations, RDGs are obliged to inject reactive current during voltage instability to aid in voltage recovery and maintain a continuous real power supply (Akinyemi et al., 2022), (Chapagain et al., 2021).

RDGs are mandated to take reactive power from the grid whenever there is a system-wide rise in reactive power. The three most important standard grid codes are the ability to ride through low voltage, the ability to control frequency, and the ability to control voltage (Tarafdar Hagh & Khalili, 2019), (Mohseni & Islam, 2012). This paper is organized as follows: Section 2 contains results and analysis, and Section 4 contains a conclusion of results work.

2. System Modelling of Wind Energy Conversion System

The power generated by a wind turbine is related to the size of the blades diameter as they move through the wind (Yossri et al., 2021). Furthermore, the output power of a wind turbine is precisely related to the cube of wind speed. Federal law prohibits wind turbine generators from having an efficiency greater than 59.9 percent (Newman, 1986), (Raju & Pillai, 2015). The following formulas demonstrate the mechanical power and rotational force that can be generated by a wind energy conversion system. The power coefficient (C_p) represents the quality of available wind energy:

$$C_p = 0.22 \left(\frac{11}{\gamma} - 0.4\beta - 5 \right) - \ell^{\frac{116}{\gamma}} \quad (1)$$

Where β denotes the pitching angle and γ denotes the tip speed ratio.

Mechanical Energy is generated by wind turbines in the following ways:

$$P_m = \frac{1}{2} * p * a * v^3 * c_p (\lambda * \beta) \quad (2)$$

Where p is the air density, v is the wind speed, a is the rotor blade area, and C_p is the power coefficient. The following equation gives the mechanical torque of the wind turbine:

$$T_m = \frac{P_m}{\omega} \quad (3)$$

2.1 Modeling of DFIG-based WECS

The WECS power converter consists of a rotor converter for controlling the generator's speed and a grid converter for injecting reactive current into the grid. The grid- connected DFIG based WECS is depicted in Figure 1.

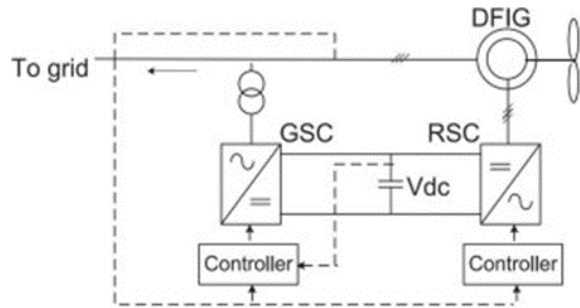


Figure 1. DFIG-based WECS(Ntuli et al., 2022).

Figures 2 and 3 show how to use a d-q reference frame to show the traditional ABC form in a DFIG.

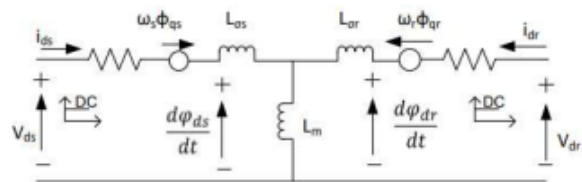


Figure 2. d-axis model of a DFIG(Ngom et al., 2018).

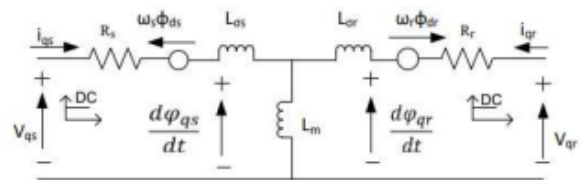


Figure 3. q-axis model of a DFIG(Ngom et al., 2018).

As depicted in figure 4, the RSC is achieved within a rotating d-q axis frame with the d-axis lined up with the position of the fixed coil flux vector.

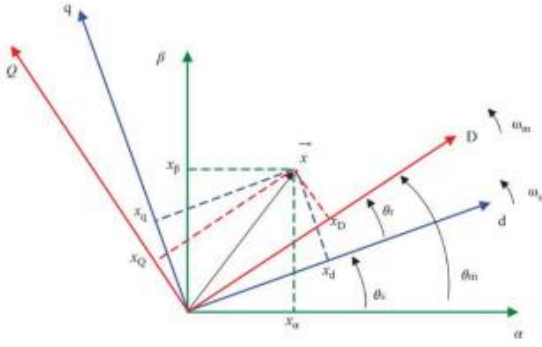


Figure 4. Three non-identical revolving reference frames(AI Zabin & Ismael, 2019).

The dynamic equations for the voltages and flux connections in a three-phase DFIG can be expressed as follows in a synchronously rotating direct-quadrature (d-q) reference frame

$$v_{ds} = r_s i_{ds} + \frac{d}{dt} \varphi_{ds} - \omega_s \varphi_{qs} \quad (4)$$

$$v_{dqs} = r_s \left| i_{qs} + \frac{d}{dt} \varphi_{qs} + \omega_s \varphi_{ds} \right. \quad (5)$$

$$Q_s = \frac{3}{2} (V_{sq} * i_{sd} - V_{sd} * i_{sq}) \quad (6)$$

$$P_s = \frac{3}{2} (V_{sd} * i_{sd} + V_{sq} * i_{sq}) \quad (7)$$

Due to the constant stator voltage, I_{qr} and I_{dr} govern the stator's active and reactive power, respectively. The rotor voltages can be expressed as a function of the rotor currents, resulting in the following formulas:

$$V_{dr} = R_r I_{dr} + \frac{d}{dt} \varphi_{dr} - \omega_r \varphi_{qr} \quad (8)$$

$$V_{qr} = R_r I_{qr} + \frac{d}{dt} \varphi_{qr} + \omega_r \varphi_{dr} \quad (9)$$

$$\varphi_{dr} = l_m * i_{ds} + l_r * i_{dr} \quad (10)$$

$$\varphi_{qr} = l_m i_{qs} + l_r i_{qr} \quad (11)$$

Where V_{ds} denotes direct-axis stator voltage, V_{qs} denotes quadrature-axis stator voltage, and I_{ds} denotes direct-axis stator current. I_{qs} denotes the current flowing through a quadrature-axis stator. L_{ds} represents stator inductance along the direct axis, L_{qs} represents stator inductance along the quadrature axis, and L_m denotes mutual inductance between the stator and rotor. R_s is the

resistance of the stator, and ω_s is its rotational frequency.

2.2 Permanent Magnet Synchronous Generator

Figure 5, depicts a grid-connected permanent magnet synchronous generator. To create a computational formula for the PMSG, the following assumptions must be made: The PMSG conductivity at zero, sinusoidal induced electromotive force, power losses at a minimum, and zero field dynamics. Nonetheless, during power system disturbances, PMS-based WECS exhibits higher DC-link voltage (Van & Ho, 2016). The following are the mathematical voltage equations:

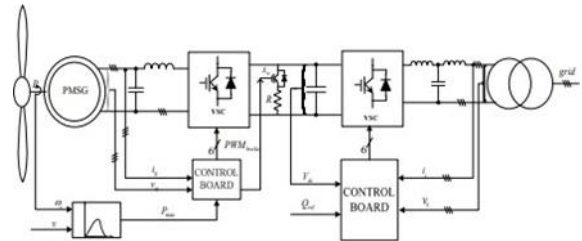


Figure 5. PMSG-based WECS(Li et al., 2010).

$$v_{ds} = -R_s i_{ds} + \omega_r L_q i_{qs} - L_d p i_{ds} \quad (12)$$

$$v_{qs} = -R_s i_{qs} - \omega_r L_d i_{ds} + \omega_r \lambda_r - L_q p i_{qs} \quad (13)$$

3. Simulation results and analysis

This section provides a comparative analysis of the two WECS topologies: i.e. the PMSG-based WECS and the DFIG-based WECS. The simulation is conducted using the MATLAB/SIMULINK. When comparing the two topologies, a single line-to-earth fault was simulated on the middle phase (white phase) of the grid transmission network for duration of 1.5 seconds. This was undertaken to compare the performance of these technologies, as the RDGs are designed to inject reactive current under unbalanced grid voltages. Figure 6 depicts the wind velocity employed in this model. The wind farm system consists of three 1.5 MW wind turbines. Both systems are shown under identical settings. The simulation for both systems was run for 12 seconds under changing wind conditions.

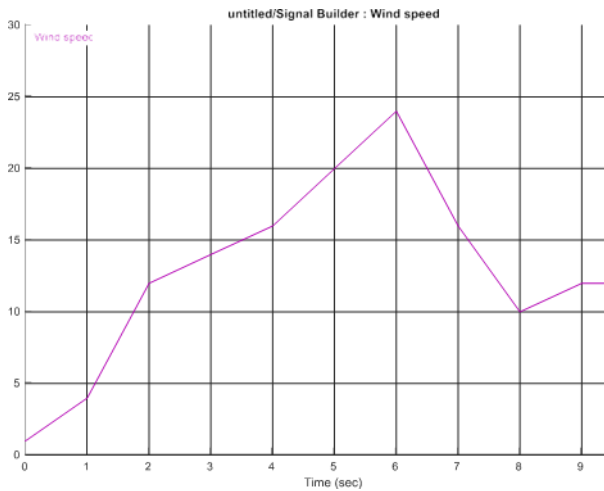


Figure 6. Wind speed signal.

Figure 7 clearly shows that there were oscillations on the active power at the startup of the PMSG. However, the overshoot was kept to a minimal. The active power in the grid was reduced to practically nil during the grid fault. As a result, it was reduced. At 5 seconds, the active power was practically at its maximum.

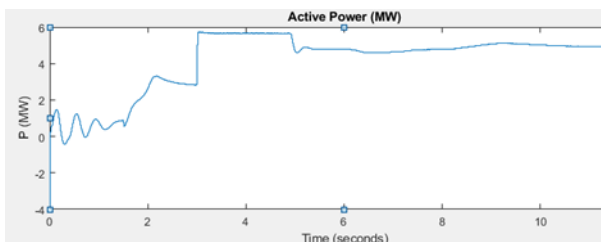


Figure 7. PMSG Active Power.

Figure 8 clearly shows that there were oscillations on the dc link voltage at initialization of the PMSG, and the increase in voltage magnitude about quadrupled the rated DC voltage. After the fault was cleared, the DC voltage was restored to its nominal value.

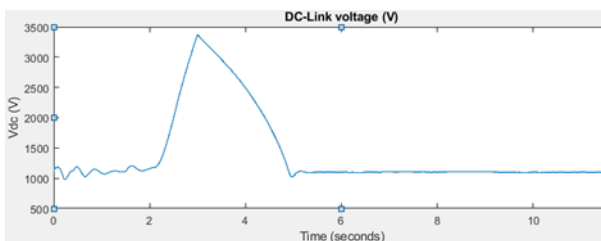


Figure 8 DC Voltage for PMSG..

Figure 9 depicts the voltage dips on the grid that were half the nominal value.

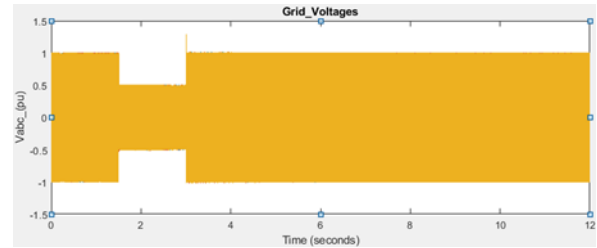


Figure 9. Grid voltage in PMSG based WECS.

Figure 10 depicts the pitch angle of the pmsg wind turbine. The pitch angle control is shown to have begun in the first 1.8 seconds of the experiment.

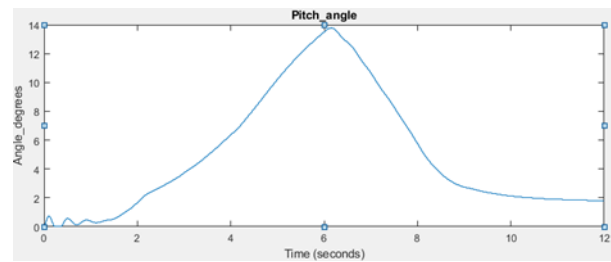


Figure 10. Pitch angle of PMSG based WECS.

Figure 11 depicts how reactive power was introduced into the grid during the fault incident. After the issue was resolved, the reactive power was reduced from 3.8 to 5 seconds of simulation time. However, after 5 seconds, it dropped below zero, suggesting grid absorption of reactive power.

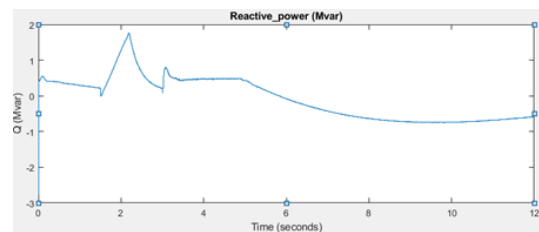


Figure 11. Reactive Power of PMSG based WECS.

Figure 12 shows that the pmsg rotor speed increased to nearly double the rated rotor speed. After 9 seconds of simulation, it was reset to its original value.

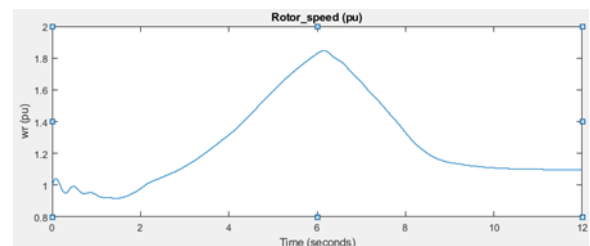


Figure 12. Rotor speed of PMSG.

Between two and five seconds, the stator voltages of the PMSG rises by one pu. And the capture results are shown in Figure 13.

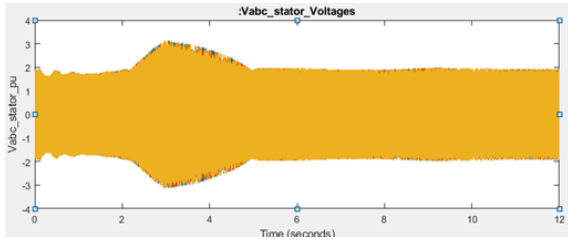


Figure 13. Stator voltage of PMSG.

Figure 14 shows that when there is a fault, the real power goes down to almost zero. Once the fault is fixed, the active power goes back to its nominal values. The optimal active power was reached in 8 seconds, and the wind farm system was working at full capacity.

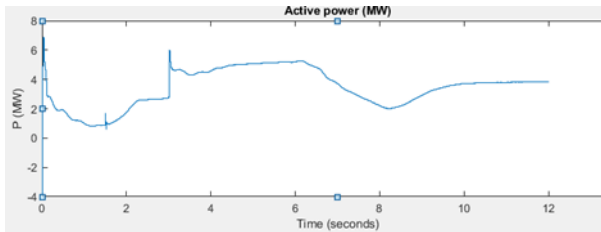


Figure 14. DFIG active power.

Figure 15 depicts the voltage dips on the grid that were half the nominal value.

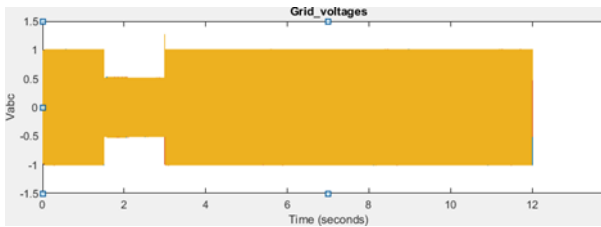


Figure 15. Grid voltages for DFIG based WECS.

Figure 16 indicates that the pitch angle control began shortly after the rotor speed exceeded its rated value and that it was disabled after 8 seconds because the DFIG was running at its optimal speed (rated speed).

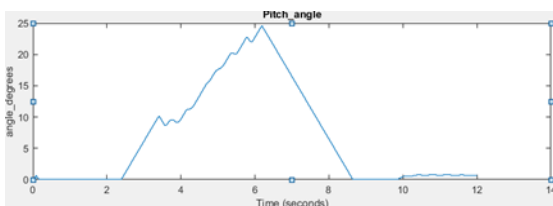


Figure 16. Pitch angle control for DFIG based WECS.

The fault-ride-through capability of the DFIG-based WECS is illustrated in figure 17. The model was capable of injecting the reactive power needed to return the power system to normal operating conditions. DFIG was able to retain zero reactive power when the fault was rectified.

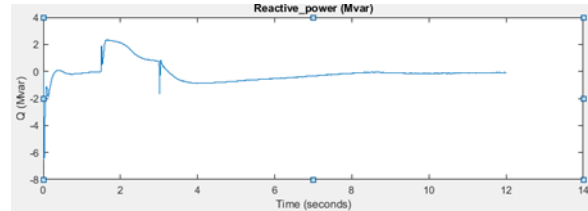


Figure 17. DFIG reactive power.

The rotor speed drooped during the grid failure, and after the fault was cleared, the rotor speed began to alter with the change in wind speed, as seen in Figure 18. The dfig was running at full speed after 10 seconds.

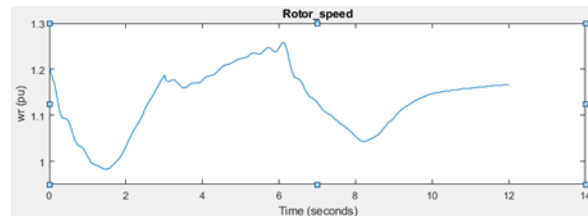


Figure 18. DFIG rotor speed.

During the fault occurrence, the DC link voltage was temporarily disrupted. It was, nevertheless, kept within the rated value as shown through Figure 19.

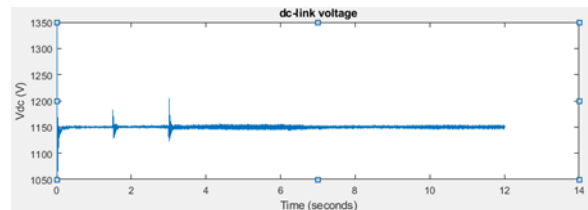


Figure 19. DFIG DC Link voltage.

Figure 20 depicts the voltage dips on the stator of DFIG that were 75 per cent the nominal value.

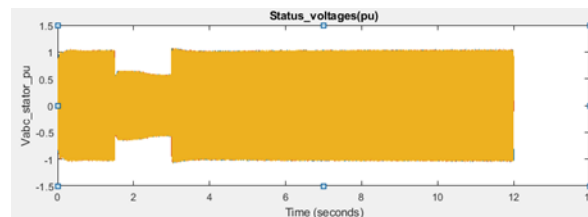


Figure 20. DFIG stator voltage.

3.1 summarized results

This section provides an analysis of the dynamic performance of a DFIG-based WECS against a PMSG-based WECS. The capability solutions for grid-coded power generation have been analyzed, and the application results of both systems have been shown under identical working conditions. The results indicate that the DFIG-based WECS topology outperformed the PMSG-based WECS topology. Table 1 compares the two topologies.

Table 1. Summarized results.

Mode I Type	DC-Link Voltage	Reactive Power (Mvar)	Active Power (MW)
DFIG-based WECS	It enables robust management of DC-link voltage during grid disruptions in terms of overshoot. As a result, generator rotor damage is prevented.	By injecting reactive power, the model excels at bolstering the grid during faults. In addition, once the problem has been rectified, the system can operate at about 0 Mvar, as required by standard grid code.	During grid faults, the active power of the system was drastically decreased, but once the fault was resolved, the system resumed normal operation. Consequently, active power has a significant impact on power system frequency.
PMSG-based WECS	The DC-link voltage is approximately three times the reference voltage. This could lead to system	The model can handle the reactive power needs of the grid. However, once the	In terms of active power supply, the model is more resilient than the recommended method. The

	destruction. It also requires additional precautions .	fault has been rectified, it cannot operate at 0 Mvar as per grid code regulations.	performance of DC-link voltage and reactive power, however, makes the DFIG-based WECS superior to the PMSG-based WECS.
--	--	---	--

4. Conclusion

This research work is dedicated to study the impact of grid disturbance on PMSG and DFIG systems. The various parameters, such as active power, DC link voltage, grid voltage, reactive power, stator voltages of PMSG and DFIG are shown in the event of the disturbance and the system results are shown for PMSG and DFIG. As a result, it is concluded that DFIG is more effective as a wind turbine generator in comparison to PMSG for a particular disturbance. The contrast can be summarized by saying that DFIG injected enough reactive power during the fault and maintained zero reactive power at the steady state condition. Furthermore, DFIG demonstrates a high level of capability in regulating DC link voltage to its nominal value when matched with PMSG under the same operating conditions. This indicates that DFIG is more stable than PMSG in the presence of varying wind speeds and, in the event of grid faults; hence it can be concluded that DFIG is more suitable and robust for wide wind speeds and for grid disturbances.

5. References

- Akinyemi, A. S., Musasa, K., & Davidson, I. E. (2022). Analysis of voltage rise phenomena in electrical power network with high concentration of renewable distributed generations. *Scientific Reports*, 12(1), 1-22.
- Al Zabin, O., & Ismael, A. (2019). Rotor current control design for DFIG-based wind turbine using PI, FLC and fuzzy PI controllers. 2019 International Conference on Electrical and Computing Technologies and Applications (ICECTA),

- Chapagain, P., Culler, M., Ishchenko, D., & Valdes, A. (2021). Stability impact of IEEE 1547 operational mode changes under high DER penetration in the presence of cyber adversary. 2021 IEEE Green Technologies Conference (GreenTech).
- Gupta, S., & Shukla, A. (2022). Improved dynamic modelling of DFIG driven wind turbine with algorithm for optimal sharing of reactive power between converters. *Sustainable Energy Technologies and Assessments*, 51, 101961.
- Li, J., Li, D., Hong, L., Xie, C., & Chen, G. (2010). A novel power-flow balance LVRT control strategy for low-speed direct-drive PMSG wind generation system. IECOn 2010-36th Annual Conference on IEEE Industrial Electronics Society.
- McKenna, R., Pfenninger, S., Heinrichs, H., Schmidt, J., Staffell, I., Bauer, C., Gruber, K., Hahmann, A. N., Jansen, M., & Klingler, M. (2022). High-resolution large-scale onshore wind energy assessments: A review of potential definitions, methodologies and future research needs. *Renewable Energy*, 182, 659-684.
- Mohseni, M., & Islam, S. M. (2012). Review of international grid codes for wind power integration: Diversity, technology and a case for global standard. *Renewable and Sustainable Energy Reviews*, 16(6), 3876-3890.
- Nadour, M., Essadki, A., & Nasser, T. (2020). Improving low-voltage ride-through capability of a multimegawatt DFIG based wind turbine under grid faults. *Protection and Control of Modern Power Systems*, 5(1), 1-13.
- Newman, B. (1986). Multiple actuator-disc theory for wind turbines. *Journal of wind engineering and industrial aerodynamics*, 24(3), 215-225.
- Ngom, I., Mboup, A. B., Dieng, A., & Diaw, N. (2018). Efficient Control of Doubly Fed Induction Generator Wind Turbine Implementation in Matlab Simulink. *Journal of Engineering Research and Application*, 8(7 (Part-I)), 06-12.
- Ntuli, W. K., Sharma, G., & Kabeya, M. (2022). Study of Fault Ride-Through Capability of Doubly Fed Induction Generator Based Wind Turbine. 2022 30th Southern African Universities Power Engineering Conference (SAUPEC).
- Olson-Hazboun, S. K. (2018). "Why are we being punished and they are being rewarded?" views on renewable energy in fossil fuels-based communities of the US west. *The Extractive Industries and Society*, 5(3), 366-374.
- Ouyang, J., Tang, T., Yao, J., & Li, M. (2019). Active voltage control for DFIG-based wind farm integrated power system by coordinating active and reactive powers under wind speed variations. *IEEE Transactions on Energy Conversion*, 34(3), 1504-1511.
- Qazi, A., Hussain, F., Rahim, N. A., Hardaker, G., Alghazzawi, D., Shaban, K., & Haruna, K. (2019). Towards sustainable energy: a systematic review of renewable energy sources, technologies, and public opinions. *IEEE Access*, 7, 63837-63851.
- Raju, S. K., & Pillai, G. N. (2015). Design and implementation of type-2 fuzzy logic controller for DFIG-based wind energy systems in distribution networks. *IEEE Transactions on Sustainable Energy*, 7(1), 345-353.
- Sewchurran, S., & Davidson, I. E. (2016). Guiding principles for grid code compliance of large utility scale renewable power plant intergration onto South Africa's transmission/distribution networks. 2016 IEEE International Conference on Renewable Energy Research and Applications (ICRERA).
- Tarafdar Hagh, M., & Khalili, T. (2019). A review of fault ride through of PV and wind renewable energies in grid codes. *International Journal of Energy Research*, 43(4), 1342-1356.
- Van, T. L., & Ho, V. C. (2016). Enhanced fault ride-through capability of DFIG wind turbine systems considering grid-side converter as STATCOM. In *AETA 2015: Recent Advances in Electrical Engineering and Related Sciences* (pp. 185-196). Springer.
- Voglitsis, D., Papanikolaou, N., & Kyritsis, A. C. (2016). Incorporation of harmonic injection in an interleaved flyback inverter for the implementation of an active anti-islanding technique. *IEEE transactions on power electronics*, 32(11), 8526-8543.
- Yossri, W., Ben Ayed, S., & Abdelkefi, A. (2021). Three-dimensional computational fluid dynamics investigation on size effect of small-scale wind turbine blades. AIAA Scitech 2021 Forum.